Journal of Thermal Analysis and Calorimetry (2023) 148:11467–11477
https://doi.org/10.1007/s10973-023-12492-8

Characterization of Al_2O_3, TiO_2, hybrid Al_2O_3-TiO_2 and graphene oxide nanofluids and their performance evaluations in photovoltaic thermal system

Saeed Rubaiee[1,2] · Syed Mohd Yahya[3] · M. A. Fazal[1] · Mohd Danish[1]

Received: 9 December 2022 / Accepted: 12 August 2023 / Published online: 31 August 2023

Abstract

Advanced nanofluid with high stability is essential to meet the demands of the current industry and solar thermal systems. In industrial application, graphene oxide (GO) nanofluid formulated with ethylene glycol (EG)/water (W) is usually well-known for good stability along with high thermal conductivity. In this research, GO nanofluid is characterized for exploring its thermal, optical and suspension stability under certain conditions and then utilized as working fluid in photovoltaic thermal (PV/T) system for measuring its performance compared to those of water and Al_2O_3, TiO_2 and hybrid Al_2O_3-TiO_2-based nanofluids. The thermal conductivity, thermal stability, morphology and optical absorbance are characterized by using thermal analyzer, TGA, SEM and UV–vis analysis, respectively. The results revealed that the thermal conductivity of GO/EG:W nanofluid was increased by 9.5% at 40 °C compared to water. It also showed good stability with a zeta potential of 30.3 mV. The numerical implantation of GO/EG:W nanofluid performed by COMSOL Multiphysics software presented significant improvement compared to Al_2O_3/EG:W, TiO_2/EG:W and TiO_2-Al_2O_3/EG:W nanofluids with a concentration of 0.01 mass% to 0.1 mass%. The measured electrical and thermal efficiencies of the PV/T system were 13.5% and 76%, respectively, using GO/EG:W with 0.07 kg s^{-1} mass flow rate and 0.01 mass% concentration. The stated findings identified GO/EG:W nanofluid as more effective in enhancing PV/T system's performance than other tested working fluids.

Keywords Graphene · Ethylene glycol · Nanofluids · PV/T · Electrical efficiency · Thermal efficiency

Abbreviations

EG	Ethylene glycol
PV	Photovoltaic
EDX	Energy-dispersive x-ray
PV/T	Photovoltaic thermal
FEA	Finite element analysis
SWCNT	Single-walled carbon nanotube
FESEM	Field emission scanning electron microscopy
TEM	Transmission electron spectroscopy
FF	Fill factor
TGA	Thermogravimetric analysis
GO	Graphene oxide
UV–vis	Ultraviolet–visible spectroscopy
GO/EG:W	Graphene oxide/Ethylene Glycol: Water
UDF	User-defined functions
I_{sc}	Short-circuit current
V_{oc}	Open-circuit voltage
MWCNT	Multi-walled carbon nanotube

✉ Saeed Rubaiee
salrubaiee@uj.edu.sa

Syed Mohd Yahya
smyahya@zhcet.ac.in

M. A. Fazal
fazal@uj.edu.sa

Mohd Danish
mdanish@uj.edu.sa

[1] Department of Mechanical and Materials Engineering, University of Jeddah, Jeddah, Kingdom of Saudi Arabia

[2] Department of Industrial and Systems Engineering, University of Jeddah, Jeddah, Kingdom of Saudi Arabia

[3] Sustainable Energy and Acoustics Research Lab, Mechanical Engineering Department, Aligarh Muslim University, Aligarh 202002, India

Introduction

The continuous growth of energy needs, environmental degradations, rising price and scarcity of fossil fuels have made it essential to explore the alternative and sustainable renewable energy sources. In this case, solar energy has emerged as one of the most potent alternative renewables, freely available everywhere to produce electricity and heat. The most efficient and sustainable technologies employed in generating electric current and heat are photovoltaic (PV) and thermal collector systems, respectively [1, 2]. The energy harnessing efficiencies of these technologies are usually observed in the range of approximately 15–20% [3] and 50–70% [4], respectively. Researchers around the world are paying tremendous efforts in augmenting the efficiencies of these systems [2, 5]. At present, the photovoltaic thermal (PV/T) system developed by integrating both PV and solar thermal systems receives considerable attention from researchers as it improves energy generation efficiency [1, 6]. It is used in several forms including solar water heating, solar desalination, solar drying and so on. The working fluid used in the PV/T system plays key role in absorbing heat from solar module and transferring it to the collector. The thermal conductivity of commonly used base fluid like oil, water or ethylene glycol is usually increased by colloidal mixture of nanoparticles (1–100 nm). The suspended nanoparticles in base fluid help improve its thermal conductivity. Thus, it increases the overall performance of the PV/T system [2]. The literature studies [2, 6] reveal that the commonly used metal-based nanoparticles in preparing nanofluids are either metal (Zn, Fe, Cu and Al) or metal oxides (Al_2O_3, ZnO, Cu_2O, TiO_2, etc.). Many researchers use carbon-based nanomaterials such as fullerenes (carbon molecule, C_n at where $n < 20$) [7], carbon nanotubes [6] and graphene (carbon with two-dimensional allotropic form) [8]. Concerning PV/T system's overall efficiency, thermal and electrical efficiency, surface temperature, entropy generation and energy loss, different researchers investigated various input parameters with nanofluids including types, shape, size and concentration of used nanoparticles, base fluid types, stability, viscosity and flow rate experimentally and numerically [9, 10].

Among various nanofluids, metal-oxide nanofluids have received more attention from researchers due to their chemical and thermal stability and long self-service life [11]. Delouei et al., [12] examined the performance of Al_2O_3/water nanofluid on heat transfer under turbulent flow with various effects of ultrasonic vibrations, and they observed heat transfer to increase up to 15.27%. They added that the ultrasonic effect played significant role in improving heat transfer rate and reducing pressure drop. Abdullah et al., [13] investigated the effect of Al_2O_3/water nanofluid with various volume fraction starting from 0.075 to 0.2% on PV/T system's performance with plate and tube collector. They reported that the reduction in the maximum and the average temperature of the module surface achieved by 0.1% Al_2O_3 with 1.2 L min^{-1} are 10 °C and 8.6 °C, respectively. Recently, an in-depth review study on TiO_2 nanofluid has been published by Yang and Hu [14]. According to them, TiO_2 nanofluid like Al_2O_3-based nanofluid has also captured researchers' attention due to its sensational dispersion characteristic, non-toxicity and chemical stability. Kilic et al. [15] investigated the efficiency of a flat plat solar collector by using water and TiO_2 (2 mass%)-based water nanofluids, and they achieved instantaneous efficiency of 36.204% and 48.672%, respectively. Similarly, Subramani et al. [16] reported that the thermal efficiency of the parabolic trough collector improved up to 8.66% due to use of TiO_2-water nanofluid. The thermal efficiency of PV/T system was drastically increased from 42.8 to 69.7% due to the use of 0.5 mass% TiO_2/water nanofluid at a flow rate of 2.5 L min^{-1} [17]. Geometry of fluid flow and types of used fluids greatly influence the efficiency of thermal collectors [18]. Samylingam et al., [19] examined the performances of Al_2O_3-water PV/T and MXene nanofluids. They observed 16% higher thermal efficiency and 9% higher heat transfer coefficient for MXene nanofluid against Al_2O_3-water-based nanofluid.

In the recent time, a good number of researchers [20, 21] examined the effect of single-walled carbon nanotube (SWCNT) and multi-walled carbon nanotube (MWCNT) nanofluids on performance of PV/T system because of their super thermal properties. Sangeetha et al., [21] examined the electrical efficiency of PV/T systems using MWCNT, Al_2O_3 and TiO_2 nanofluids. They reported the electrical efficiency to increase up to 47%, 33% and 27%, respectively. Like other nanofluids, investigations on graphene nanofluid have captured a rapidly increasing trend. Venkatesh et al., [22] reported that the use of water-based graphene nanofluids improved energy efficiency of PV/T system. They observed the module surface temperature to decrease by approximately 20 °C and increase the electrical and thermal efficiency by 23% and 13%, respectively. In fact, graphene-based nanofluids are reported for their outstanding conductivity, high ratio of surface area to volume, high suspension stability and good thermophysical properties with improved heat transfer property [23]. However, water-based graphene is reported for its poor stability due to having hydrophobic nature [24]. Some researchers utilized ethylene glycol or a mixture of ethylene glycol plus water in preparing graphene nanofluids [23, 24].

The above literature study demonstrates that the type of heat collecting fluids employed in PV/T system and their properties are the prime factors toward unlocking its improved efficiency. The use of various advanced nanofluids with PV/T system usually enhances the overall efficiency at different levels; however, change in flow rates, because of its impacts on heat transfer coefficient, thermal and electrical efficiencies, can be challenging for different nanofluid-based PV/T systems. It was also found from the literatures that the use of carbon-based nanofluid showed better performances as compared to other nanofluids. However, graphene-based carbon nanofluids were not sufficiently studied. Very few studies are available to explore its characteristics such as thermal conductivity, optical absorbance, stability, specific heat capacity, viscosity, and PV/T performances. In addition, theoretical works exploring the heat transfer mechanism is crucial as any single property of nanofluids cannot determine the efficiency of heat transfer in the system. The limited information on thermophysical properties for various nanofluids represents significant gap between fundamental research and practical applications in regulating thermal heat management. Hence, the present study aims to prepare various nanofluids by dispersion of graphene oxide, alumina, titania and hybrid Al_2O_3-TiO_2 in ethylene glycol–water and compare their characteristics and performances with the PV/T system.

Experimental

Preparation of aqueous ethylene glycol nanofluids

Graphene nano-platelets used in preparing nanofluids were procured from the SRL laboratory. These graphene nano-platelets were dispersed in water/ethylene glycol (60:40 volumetric ratio) by keeping the mass faction from 0.1% to 0.3%. The required mass of the graphene nano-platelets weighed with the help of calibrated digital balance. At the next stage, one-kilogram water–ethylene glycol in the ratio of 60:40 by volume was prepared. A surfactant (NPE 400) in volumetric ratio of 0.1% of the base fluid is added to achieve maximum stability of nanofluid. A speed stirrer rotating at around 300 rpm was used to disperse the graphene nano-platelets in water–ethylene glycol solution. The stirrer runs for about 20 min to achieve a high level of nanofluid stability. The nanofluid prepared by the stirrer might have agglomerations of nanoparticles. Hence, to break these agglomerations, an ultrasonic homogenizer was used. There might be chances of damage of nano-platelets, so to minimize this damage, the sonication of nanofluid was performed for 10 min at 20 kHz and 150 Watt.

UV–Vis analysis of the aqueous ethylene glycol nanofluids

Ultraviolet–visible spectroscopy (UV–Vis) (PerkinElmer Lambda 750) was used to record optical absorbance at room temperature for a wavelength within 800–200 nm. The scan speed was adjusted at 266.75 nm min^{-1} with 860 nm.

Viscosity measurement of aqueous ethylene glycol nanofluids

The viscosity of different working fluid was measured by using a viscosity analyzer (Rheometer Anton Paar model MCR92). T-Ramp (e.g., viscosity variation with temperature) was measured within 20–80 °C for all samples. T-Ramp measurements for the pure aqueous ethylene glycol and aqueous ethylene glycol nanofluids including four different types of nanoparticles and in different concentrations were performed in identical condition to assure the uniformity of the measurements.

Microstructure and morphological analysis of graphene

The morphology of the synthesized graphene nanoflakes was monitored with a scanning electronic microscopy (SEM) having a model of TESCAN, VEGA3 and energy-dispersive spectroscopy (EDS). The platinum (Pt) coating for each sample was developed by using a digital iron coater (SPT-20).

Thermal stability measurement

PerkinElmer TGA 4000 was used for the thermogravimetric analysis of the synthesized nanofluids. A 180-μL alumina crucible capable of withstanding a temperature of ~ 1750 °C was used. The 2.6 bar pressure was used for the gas flowing at a 19.8 mL min^{-1} rate to raise the selected temperature. The decomposition temperature was measured by using around 10 mg synthesized nanofluid. The temperature range and rate of change were 30–400 °C and 10 °C min^{-1}, respectively.

Thermal conductivity measurement

The property of thermal conductivity of synthesized aqueous ethylene glycol nanofluids with different concentrations was measured with the help of thermal properties analyzer (Tempos) via improved proprietary algorithm. The sensor of the analyzer was KS-3 with a length of 60 mm and a diameter of 1.3 mm. The selected sensor could measure the thermal conductivity within 0.02–2 W m^{-1} K^{-1} with an accuracy of ± 10%. Thermal conductivity measurements for all prepared samples were executed at four different temperatures including 25 °C, 40 °C, 55 °C and 70 °C. Firstly, the prepared samples were poured into a vial followed by locating the KS-3 sensor inside the sample. Then, the vial was placed inside a water bath (MEMMERT, WNB22) for stabilizing the temperature to achieve accurate results. Thermal conductivity measurements for all samples in certain temperatures were repeated for 5 times to ensure the accuracy of the obtained data.

Thermal and electrical performances in PV/T system

The thermal and electrical performance of mono- and hybrid nanofluids was numerically investigated using COMSOL, and their performances were compared with those of graphene-based aqueous ethylene glycol nanofluids. Multiphysics simulation software was used for modeling and simulation. Since this software was based on the FEM methodology, results were more accurate with less numerical error. Furthermore, this software could deal with complex geometry as well.

Physical model of PV/T system

In the case of the PV/T system, different researchers employed various active and passive techniques to control the temperature rise in the PV module. Many of them control the of PV module's temperature by using coolant (nanofluid) at the back of the PV panel. The cooling from back of the PV module is predominantly employed in hot arid climate to achieve better electrical efficiency. For this part, a numerical study was carried out to examine the performance of four EG:W-based nanofluids; Al_2O_3, TiO_2, hybrid Al_2O_3-TiO_2 and graphene integrated PV/T system in a concentration range of 0.01 mass% to 0.1 mass%. The performances of PV/T systems integrated with all four nanofluids were investigated and compared with water-based PV/T system numerically. Figure 1 presents the block diagram of the experimental work conducted in preparing different nanofluids, evaluating their properties and performances with PV/T system.

Numerical modeling of PV/T system

To investigate the performance of PV/T system numerically, COMSOL, a finite element-based software is used. The flow of nanofluid is assumed to be steady, incompressible, laminar and three-dimensional. The mixture of nanoparticle in base fluid is assumed homogeneous indicating no agglomeration

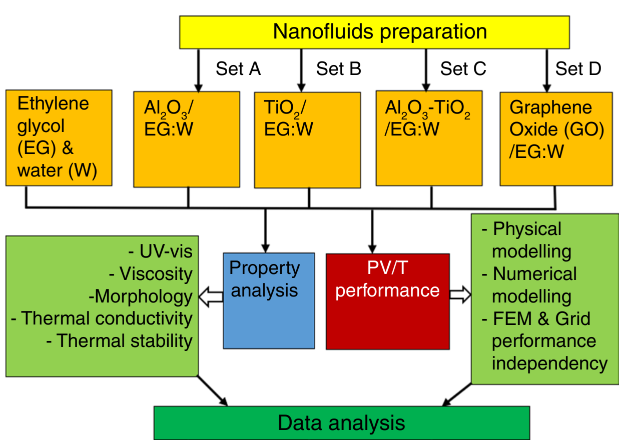

Fig. 1 Block diagram of the experimental work conducted for preparing different nanofluids, evaluating their properties and performances with PV/T system

of nanoparticles in it. In this study, Al_2O_3, TiO_2 and hybrid Al_2O_3-TiO_2 nanoparticles with 1.5 mass% concentration are used. The thermal conductivity corresponds to 1.5 mass% nanoparticle concentration which shows maximum value; therefore, this concentration with different temperature is incorporated into a polynomial of third order using regression analysis, and then numerical relations so obtained is inserted to COMSOL environment by user-defined function. Graphene-based nanofluid of 0.1% concentration with different temperature is incorporated into a polynomial of third order using regression analysis, and then numerical relations so obtained is again inserted to COMSOL. The numerical modeling of viscosity for all four nanofluids as a function of temperature is obtained by regression analysis of the data received experimentally. Then, the equation obtained is fitted in COMSOL by using UDF likewise thermal conductivity and used for simulation purpose. The continuity, momentum and energy equations (Eqs. 1–5) that describe the flow are as follows:

Continuity:

$$\frac{\partial u}{\partial x}+\frac{\partial v}{\partial y}+\frac{\partial w}{\partial z}=0 \tag{1}$$

X-momentum:

$$\rho_{\mathrm{nf}}\left(u\frac{\partial u}{\partial x}+v\frac{\partial u}{\partial y}+w\frac{\partial u}{\partial z}\right)=\frac{-\partial P}{\partial x}+\mu_{\mathrm{nf}}\left(\frac{\partial^2 u}{\partial x^2}+\frac{\partial^2 u}{\partial y^2}+\frac{\partial^2 u}{\partial z^2}\right) \tag{2}$$

Y-momentum:

$$\rho_{\mathrm{nf}}\left(u\frac{\partial v}{\partial x}+v\frac{\partial v}{\partial y}+w\frac{\partial v}{\partial z}\right)=\frac{-\partial P}{\partial y}+\mu_{\mathrm{nf}}\left(\frac{\partial^2 v}{\partial x^2}+\frac{\partial^2 v}{\partial y^2}+\frac{\partial^2 v}{\partial z^2}\right) \tag{3}$$

Z-momentum:

$$\rho_{\mathrm{nf}}\left(u\frac{\partial w}{\partial x}+v\frac{\partial w}{\partial y}+w\frac{\partial w}{\partial z}\right)=\frac{-\partial P}{\partial z}+\mu_{\mathrm{nf}}\left(\frac{\partial^2 w}{\partial x^2}+\frac{\partial^2 w}{\partial y^2}+\frac{\partial^2 w}{\partial z^2}\right) \tag{4}$$

Energy equation:

$$\rho_{\mathrm{nf}}C_{\mathrm{Pnf}}\left(u\frac{\partial T}{\partial x}+v\frac{\partial T}{\partial y}+w\frac{\partial T}{\partial z}\right)=K_{\mathrm{nf}}\left(\frac{\partial^2 T}{\partial x^2}+\frac{\partial^2 T}{\partial y^2}+\frac{\partial^2 T}{\partial z^2}\right) \tag{5}$$

The density (ρ) and heat capacitance (C_p) of nanofluids are assumed constant, and these values are calculated with the help of empirical correlations available in the literature as follows (Eqs. 6 and 7):

$$\rho_{nf} = (1 - \phi)\rho_f + \phi\rho_s \quad (6)$$

$$Cp_{nf} = (1 - \phi)\left(C_P\right)_f + \phi\left(C_P\right)_s \quad (7)$$

Equation 8 gives the energy balance applied across the PV/T system. This equation consists of convection between PV/T system and ambient (Q'_{conv}), radiation from the panel surface ($Q'rad$), and irradiance from the sun (G), the electrical power output (P_{el}) and the thermal power (P_{th}) generated.

$$G - P_{el} - P_{th} - Q'_{conv} - Q'_{rad} = 0 \quad (8)$$

The radiative and convective heat emery transfer from PVT system is given by Eqs. 9 and 10:

$$-n.(-k\nabla T) = h\left(T_{amb} - T\right) \quad (9)$$

$$-n.(-k\nabla T) = \varepsilon\sigma\left(T^4_{amb} - T^4\right) \quad (10)$$

The electrical and thermal power output of the hybrid PVT system are calculated by using Eqs. 11 and 12, respectively. The electrical power (P_{el}) output depends on open-circuit voltage (V_{oc}), short-circuit current (I_{sc}) and fill factor (FF), while the thermal power (P_{th}) generated is mainly controlled by the temperature difference.

$$P_{el} = V_{oc} * I_{sc} * FF \quad (11)$$

$$P_{th} = mC_p\left(T_{out} - T_{inn}\right) \quad (12)$$

The calculation of electrical (η_{el}) and thermal (η_{th}) efficiencies of the hybrid PV/T system can be presented by Eqs. 13 and 14, respectively.

$$\eta_{el} = \frac{P_{el}}{G * A_c} \quad (13)$$

$$\eta_{th} = \frac{P_{th}}{G * A_c} \quad (14)$$

Boundary conditions

The adiabatic condition is employed for the side surfaces of the system, while no slip condition is used for solid boundaries. The concept of heat flux continuity is applied at the fluid–solid interface. The zero-pressure boundary condition is employed at the outlet, while at inlet, $v = V_o$, $u = 0$, $w = 0$ and $T = T_o$. The bottom of the hybrid PV/T system panel was insulated.

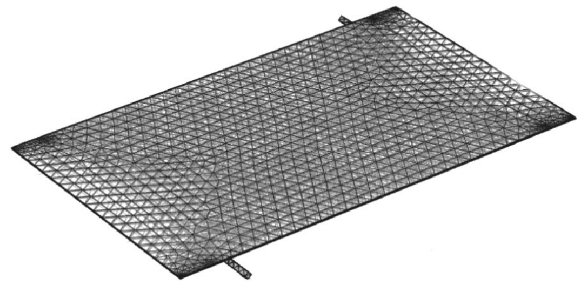

Fig. 2 PV/T model with finite element meshing

Table 1 Meshing size for grid performance independency test

S. No	Mesh size (no. of elements)	Cell temperature/°C
1	2.5×10^5	42.341
2	4×10^5	43.872
3	6×10^5	44.003
4	8×10^5	44.118
5	1.5×10^6	45.200
6	3.5×10^6	45.201

Finite element meshing and grid performance independency

The finite element meshing of the PV/T system consisting of tetrahedral and triangular mesh element at sub-domain and boundary, respectively, is presented is Fig. 2. The grid performance independency simulation at mass flow rate of 0.05 kg s^{-1} under 1000 W m^{-2} was performed using water as coolant with various mesh size shown in Table 1. It was found that there was no change in cell temperature after the mesh number 5. Therefore, mesh 5 is selected for the simulation profiles presented in this study.

Results and discussions

The FESEM and TEM images of graphene oxide (GO) nanoflakes and GO-based aqueous nanofluids are presented in Fig. 3. Upon formulation of GO nanofluid with E:W, the GO particles show surface wrinkling and well-dispersed distribution in the fluid.

Figure 3a illustrates the FESEM micrographs of GO nanoflakes, while Fig. 3b displays the surface wrinkling of GO-based aqueous nanofluids. Similarly, dispersed and transparent sheets of GO identified by TEM are presented

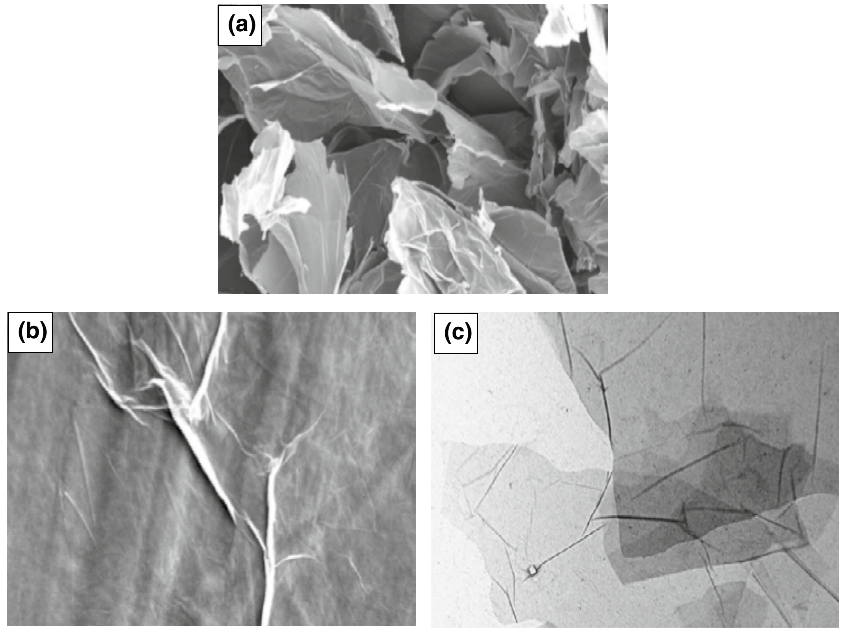

Fig. 3 **a** FESEM image of graphene oxide (GO) nanoflakes, **b** FESEM and **c** TEM images of GO-based aqueous nanofluids

in Fig. 3c. It is worth mentioning that the absolute zeta potential values for stable, limited stable and rapid aggregation are presented at > 30 mV, < 20 mV and < 5 mV, respectively. Thus, the prepared GO nanofluid is physically stable, and its zeta potential dropped to 30.3 mV only after 6 months.

Thermal conductivity analysis

The thermal conductivities of different nanofluids such as Al_2O_3, TiO_2, hybrid Al_2O_3-TiO_2 and graphene in the aqueous EG:W at 0.1% concentrations and aqueous EG:W are presented in Fig. 4. Among others, the GO nanofluid shows higher thermal conductivity.

The order of thermal conductivity shown in Fig. 4 is GO/EG:W > TiO_2-Al_2O_3/EG:W > Al_2O_3/EG:W > TiO_2/EG:W > EG:W. The thermal conductivity of EG:W is increased from 0.32 to 0.44 W m^{-1} K^{-1} at 25 °C due to the addition of graphene oxide. It is also seen from Fig. 4 that the thermal conductivity rises linearly with increasing temperature. The thermal conductivity of GO nanofluid is raised from 0.44 to 0.5 W m^{-1} K^{-1} when temperature is increased from 25 to 70 °C. The temperature grows at the same rate for each temperature step. The cause of this phenomenon can be related to Brownian motion of the particles in the nanofluid [25–27]. When temperature increases, the kinetic energy of the nanoparticle inside the nanofluid also increases leading to faster collision among the nanoparticles. Hence, the thermal conductivity is enhanced as reported by Tiwari et al. [28] and Sandhya et al. [29]. In the present study, a linear enhancement in thermal conductivity is observed with the increase in temperature. This is in good agreement with the findings reported in the literatures [25, 27].

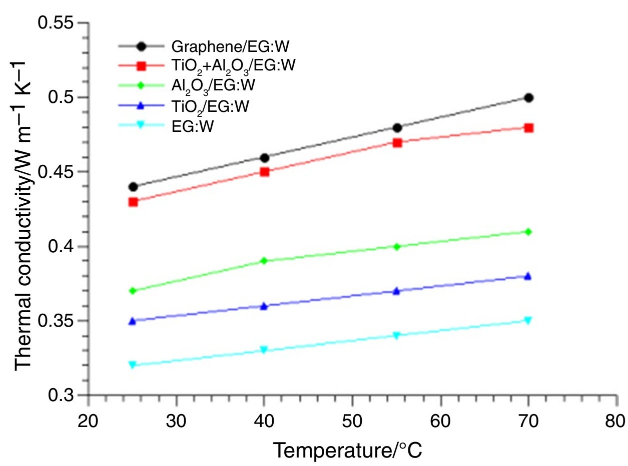

Fig. 4 Comparative thermal conductivity analysis of different nanofluids with increasing temperature for 0.1 mass% concentration

Thermogravimetric analysis (TGA)

The TGA analysis of different nanofluids is illustrated in Fig. 5 at an increasing temperature from nearly 30 °C to 400 °C. Approximately, 7 mg sample was taken for this analysis. The increasing rate of temperature was observed by 10 °C min^{-1}. Every material in initial stage resists to change in mass to avoid thermal degradation. Later, thermal degradation and oxidation are observed with consistent increment in temperature. The stability is assessed by the

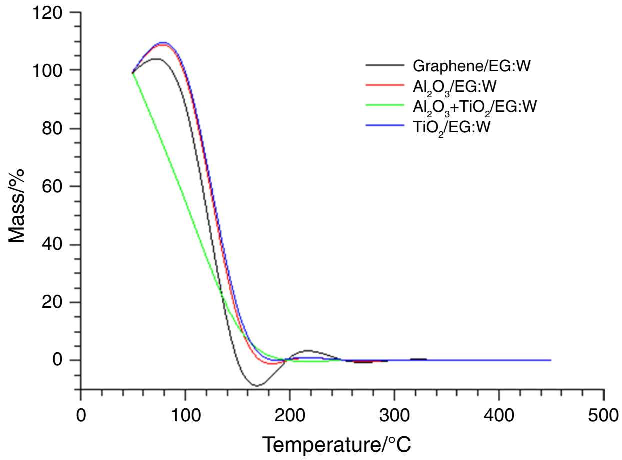

Fig. 5 Thermal degradation of nanofluids with increasing temperature at a particular concentration of 0.1 mass%

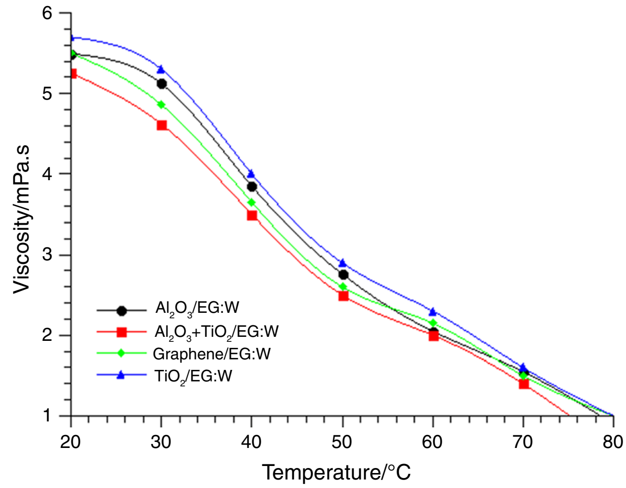

Fig. 6 Viscosity variation of different nanofluids with increasing temperature at a concentration of 0.1mass%

transition point or the temperature point where the liquid material begins to lose its mass. The thermal degradation for almost all the nanofluids begins nearly at 55 °C to 70 °C. In this temperature range, 3 to 10% of mass is lost. Water and other volatile compounds in the mixture of EG evaporate at temperature below 100 °C. However, the mass loss becomes marginal as the evaporation process initiates.

When the temperature increases, the loss of mass rapidly increases showing the degradation point. Such behavior of thermal degradation with the increase in temperature is reported by several researchers [30, 31]. At lower concentrations, the particle interaction is less, and the chance of agglomeration is also less. The thermal degradation at initial concentration of 0.1 mass% is high, and then it reduces with the increase in particle concentration and remains nearly the same for higher concentrations.

Viscosity analysis

The viscosity of the nanofluids concerning temperature and mass% concentration of the nanoparticles is depicted in Fig. 6. The temperature is varied from 20 to 80 °C in 50 steps. The variation of viscosity is significant as the nanofluids are under constant flow conditions. During such applications, the rheological properties remain intact. It is evident from Fig. 6 that the viscosity of the nanofluids is marginally affected by the concentration of the nanoparticles, while the temperature has shown a promising effect. Figure 6 presents a comparative analysis of all four nanofluids with the lowest viscosity compared to the base fluid. The hybrid nanofluid has provided the lowest viscosity at almost the same temperatures, and the TiO_2 nanofluid has a comparatively higher viscosity than others. The order of viscosity within 30–50 °C is TiO_2/EG:W > Al_2O_3/EG:W > GO/EG:W > TiO_2-Al_2O_3/EG:W.

From an overall analysis of the thermal and viscosity property of the nanofluids, the hybrid nanofluid has shown more promising result than those of individual nanoparticles suspended in the base fluid. Irrespective of nanoparticle usage at temperatures above room temperature (~ 50 °C), the increase/decrease in viscosity is found to seize. However, the viscosity remains same for all concentrations nearly at boiling point of water.

Performance of nanofluid in PV/T system

In general, the performance of the PV system decreases with the increase in its surface temperature [32, 33]. In this study, the temperature of the PV panel is reduced by using different coolants at the back of the PV panel. Figure 7a presents the variation of PV cell surface temperature for different mass flow rates of nanofluids. A significant variation in PV surface temperature is observed for mass flow rate more than 0.015 kg s^{-1}. However, the temperature of the PV cell is significantly decreased for the mass flow rate beyond 0.015 kg s^{-1}. This is due to the increase in the convection rate of heat transfer from the module with an increase in mass flow rate. For maximum mass flow rate of 0.07 kg s^{-1}, the temperature of the PV surface with TiO_2/EG:W, Al_2O_3/EG:W and Al_2O_3-TiO_2/EG:W is found to be 47 °C, 43.5 °C and 39 °C, respectively. These cell temperature values are very close to the finding (47.76 °C) reported by Rahman et al. [34]. The variation of the heat transfer coefficient with different mass flow rate is shown in Fig. 7b. The graph shows that the heat transfer coefficient increases with mass flow rate irrespective of the type of fluid used in this study. A maximum enhancement of 22% is recorded for mass flow rate of 0.06 kg s^{-1} for Al_2O_3-TiO_2/EG:W relative to the water-based PV/T system.

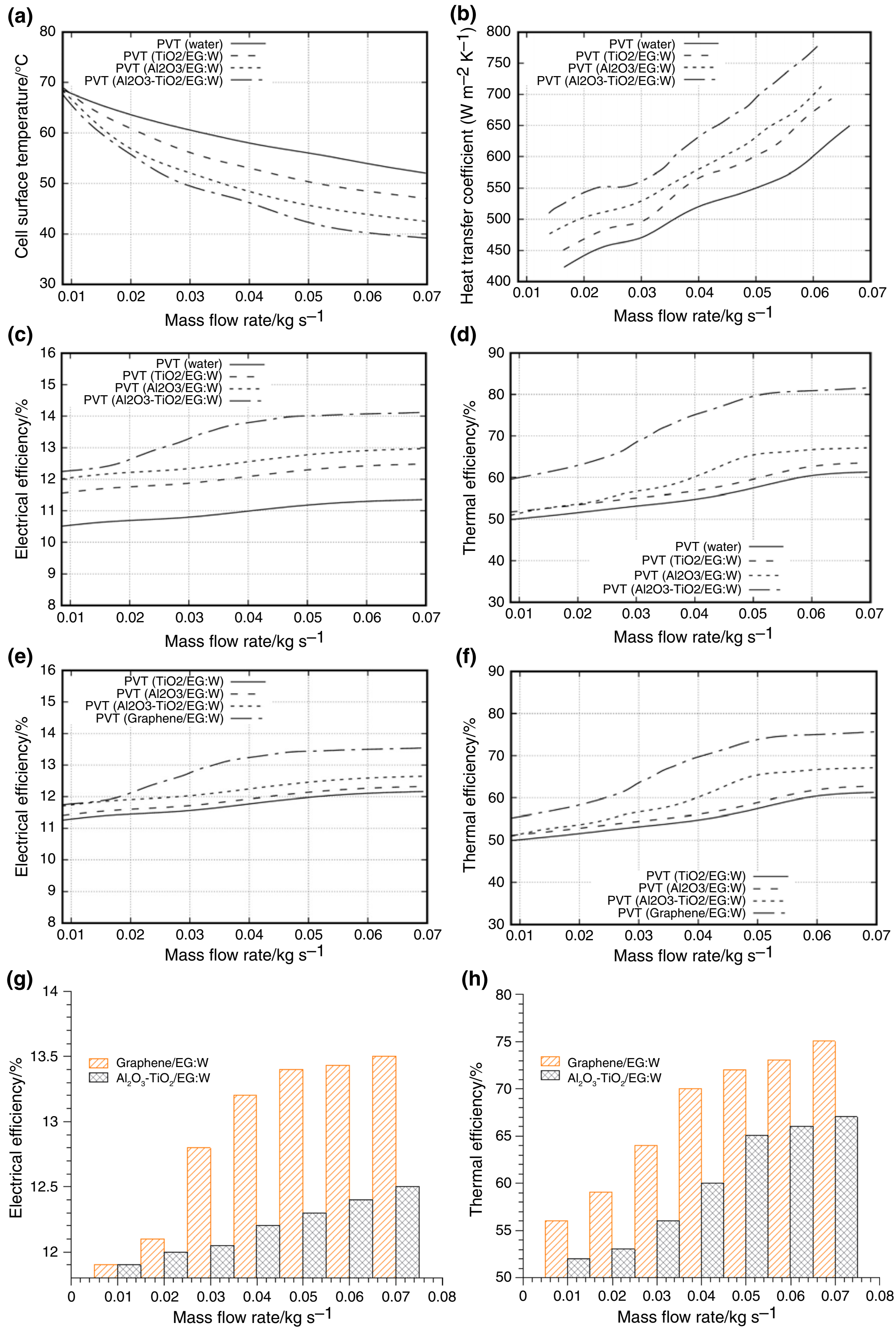
(a)
Cell surface temperature/°C
PVT (water)
PVT (TiO2/EG:W)
PVT (Al2O3/EG:W)
PVT (Al2O3-TiO2/EG:W)
Mass flow rate/kg s−1
(b)
Heat transfer coefficient (W m−2 K−1)
PVT (water)
PVT (TiO2/EG:W)
PVT (Al2O3/EG:W)
PVT (Al2O3-TiO2/EG:W)
Mass flow rate/kg s−1
(c)
Electrical efficiency/%
PVT (water)
PVT (TiO2/EG:W)
PVT (Al2O3/EG:W)
PVT (Al2O3-TiO2/EG:W)
Mass flow rate/kg s−1
(d)
Thermal efficiency/%
PVT (water)
PVT (TiO2/EG:W)
PVT (Al2O3/EG:W)
PVT (Al2O3-TiO2/EG:W)
Mass flow rate/kg s−1
(e)
Electrical efficiency/%
PVT (TiO2/EG:W)
PVT (Al2O3/EG:W)
PVT (Al2O3-TiO2/EG:W)
PVT (Graphene/EG:W)
Mass flow rate/kg s−1
(f)
Thermal efficiency/%
PVT (TiO2/EG:W)
PVT (Al2O3/EG:W)
PVT (Al2O3-TiO2/EG:W)
PVT (Graphene/EG:W)
Mass flow rate/kg s−1
(g)
Electrical efficiency/%
Graphene/EG:W
Al2O3-TiO2/EG:W
Mass flow rate/kg s−1
(h)
Thermal efficiency/%
Graphene/EG:W
Al2O3-TiO2/EG:W
Mass flow rate/kg s−1

◂**Fig. 7** Variations of **a** PV cell surface temperature and **b** coefficient of heat transfer with mass flow rate of different coolants (having 1.5 mass% concentration) under irradiance of 1000 W m^{-2}; effect of mass flow rate of different coolants having **c**, **d** 1.5 mass% and **e**, **f** 0.1 mass% concentrations on **c**, **e** electrical and **d**, **f** thermal efficiencies of PV/T systems under irradiance of 1000 W m^{-2}; **g** electrical and **h** thermal efficiency of PV/T system for different mass flow rate for comparison of Al_2O_3-TiO_2/EG:W and graphene/EG:W at 1000 W m^{-2} irradiance level and 0.1 mass% concentration

Figure 7 shows the effect of water, Al_2O_3/EG:W, TiO_2/EG:W and the hybrid of Al_2O_3-TiO_2/EG:W nanofluids on electrical and thermal efficiencies of the PV/T system by varying mass flow rate under irradiance of 1000 W m^{-2}. It is seen from Fig. 7a that the electrical efficiency increases with the increase in mass flow rate. It increases for Al_2O_3/EG:W from 11.65 to 12.5%, for TiO_2/EG:W, it increases from 12 to 13%, and for the hybrid of Al_2O_3-TiO_2/EG:W, it increases from 12.25 to 14.10% for changing the mass flow rate from 0.01 to 0.07 kg s^{-1}. Hence, by using Al_2O_3-TiO_2/EG:W nanofluid in the PV/T system, a 15.19% and 11.6% improvement in electrical efficiency is achieved in comparison with alumina and titania-based PV/T system, respectively, at 0.07 kg s^{-1} mass flow rate of nanofluids. Furthermore, 19.43% improvement in electrical efficiency using Al_2O_3-TiO_2/EG:W for 0.07 kg s^{-1} mass flow rate is achieved as compared to water as coolant. Figure 7d shows that the thermal efficiency of PV/T system increases with the increase in mass flow rate of nanofluids, irrespective of the type of nanofluids. At mass maximum flow rate of 0.07 kg s^{-1}, the thermal efficiencies of the PV/T system are 62% and 68% when water and Al_2O_3/EG:W, respectively, are used as the coolant. The thermal efficiency of PV/T system becomes 64% and 81.5%, respectively, when TiO_2/EG:W and Al_2O_3-TiO_2/EG:W are used as coolant. It is concluded from the results that Al_2O_3-TiO_2/EG:W is performing better than Al_2O_3/EG:W and TiO_2/EG:W and has high heat transfer efficiency. The thermal efficiency of the PV/T system increased by 23.9% when Al_2O_3-TiO_2/EG:W was used as a coolant instead of water.

GO/EG:W is costly and that is why low concentration is chosen, and its performance is compared with that of TiO_2/EG:W, Al_2O_3/EG:W and Al_2O_3-TiO_2/EG:W at same concentration level. Figure 7e and f presents the electrical and thermal efficiencies of PV/T with different nanofluids having a nanoparticle concentration of 0.1 mass% in the base fluid. The electrical efficiencies observed for the PV/T with TiO_2/EG:W, Al_2O_3/EG:W, Al_2O_3-TiO_2/EG:W and GO/EG:W are 12.2%, 12.3%, 12.5% and 13.5%, respectively, at the maximum flow rate of 0.07 kg s^{-1}. Similarly, the thermal efficiencies observed at the same flow rate for those systems are 62%, 64%, 68% and 76%, respectively. Both electrical and thermal efficiencies for GO/EG:W nanofluid is better than other tested fluids. It is worth to mention that Nasrin et al. [35] used MWCNT/water nanofluid and performed simulation at 0.1% concentration under 1000 W m^{-2} irradiance level. According to them, the observed electrical and thermal efficiencies were 11.96% and 73.5%. The results obtained in the current study is quite promising as compared to the findings reported by Nasrin et al. [35]. However, a little discrepancy observed could be attributed to the differences in design and nanofluid used.

Figure 7g and h illustrates the electrical and thermal efficiencies of the PV/T systems integrated with Al_2O_3-TiO_2/EG:W and graphene/EG:W at 0.1 mass% concentration and different flow rates under the irradiance of 1000 W m^{-2}. The electrical and thermal efficiencies of PV/T with GO/EG:W is 11.9% and 56%, respectively, when the flow rate is 0.01 kg s^{-1}, which are increased to13.5% and 75%, respectively, when the flow rate is 0.07 kg s^{-1}. It indicates that both electrical and thermal efficiencies of PV/T with GO/EG:W are increased with the increase in fluid flow rate. It is also found from Fig. 7g that the electrical efficiency at a higher flow rate is significantly increased for GO/EG:W PV/T as compared to Al_2O_3-TiO_2/EG:W. However, the thermal efficiency is increased significantly for GO/EG:W PV/T as compared to Al_2O_3-TiO_2/EG:W at every flow rate. This clearly indicates that Graphene/EG:W performs better than Al_2O_3-TiO_2/EG:W hybrid nanofluid. Although the current work presents a new insight into the electrical and thermal efficiencies of a PV/T system integrated with innovative GO/EG:W nanofluid, additional research is required to explore the capacity of this design in more realistic engineering applications through development of an experimental prototype.

The novelty of the present work

The current research presents a new design and develop a PV/T solar collector for better heat transfer, solve the model numerically by using FEM-based software COMSOL Multiphysics, validate numerical results with experiment, compare the thermal performance of PV/T operated by non-hybrid and carbon-based nanofluid with traditional fluid-based PV/T systems. The highest electrical and thermal efficiencies are presented by the PV/T with GO/EG:W nanofluid. These are further increased when the concentration level is increased. These results are in good agreement with the findings reported by a couple of researchers [34, 35]. The average cell temperature obtained in the current study is very close to the results reported by Rahman et al. [34]. The electrical and thermal efficiencies are validated with Nasrin et al. [35], in which they used MWCNT/water nanofluid and perform simulation at 0.1% concentration and 1000 W m^{-2} irradiance level. Our results are quite promising with these studies. However, there is a little discrepancy due to having differences in design and used nanofluids.

Conclusions

The following conclusions are drawn from the study:

1. The FESEM image of GO nanoflakes before processing shows an agglomeration of large micrometer-scale sheets displaying surface wrinkling and folding. Upon formulation of GO nanofluid, the GO particles display surface wrinkling and well-dispersed distribution in fluid. It was physically stable as the zeta potential even after 6 months was around 30.3 mV which was greater than the required value (30 mV) assigned for stability.
2. The order of thermal conductivity for the tested fluids is GO/EG:W > TiO_2-Al_2O_3/EG:W > Al_2O_3/EG:W > TiO_2/EG:W > EG:W. The thermal conductivity of EG:W is increased from 0.32 to 0.44 W m^{-1} K^{-1} at 25 °C due to the addition of graphene oxide. The thermal conductivity of GO nanofluid is further raised from 0.44 to 0.5 W m^{-1} K^{-1} when the temperature is increased from 25 to 70 °C.
3. The thermal degradation for almost all the nanofluids begins nearly at 55 °C to 70 °C. Approximately, 3 to 10% of the mass is lost in this temperature range. The viscosity is decreased with the increase in temperature, and the order of viscosity within 30–50 °C is found to be TiO_2/EG:W > Al_2O_3/EG:W > GO/EG:W > TiO_2-Al_2O_3/EG:W.
4. The electrical efficiencies observed for the PV/T with TiO_2/EG:W, Al_2O_3/EG:W, Al_2O_3-TiO_2/EG:W and GO/EG:W are 12.2%, 12.3%, 12.5% and 13.5%, respectively, at 0.1% concentration level and maximum fluid flow rate of 0.07 kg s^{-1}. Similarly, the thermal efficiencies observed for those systems at the same flow rate are 62%, 64%, 68% and 76%, respectively. This demonstrates that both electrical and thermal efficiencies for GO/EG:W nanofluid are better than other tested fluid. These efficiencies for GO/EG:W nanofluid are further increased when the concentration level is increased.
5. Both electrical and thermal efficiencies increase with the increase in mass flow rate. The electrical efficiency for Al_2O_3/EG:W, TiO_2/EG:W and Al_2O_3-TiO_2/EG:W increases from 11.65 to 12.5%, 12 to 13% and 12.25 to 14.10%, respectively, for the increase in mass flow from 0.01 to 0.07 kg s^{-1}. Similarly, the thermal efficiencies of these working fluids are increased from 62 to 64%, 64 to 68% and 68 to 81.5%, respectively, when the mass flow rate is increased from 0.01 to 0.07 kg s^{-1}. All the analyzed properties and performances of different nanofluids indicate GO/EG:W as a better-working fluid for PV/T than other tested fluids.

Acknowledgements This work was funded by the Deanship of Scientific Research (DSR), University of Jeddah, Jeddah (Grant No. UJ-02-004-ICGR). The authors gratefully acknowledge the technical and financial support of DSR.

References

1. Tembhare S, Barai D, Bhanvase B. Performance evaluation of nanofluids in solar thermal and solar photovoltaic systems: a comprehensive review. Renew Sust Energ Rev. 2022;153:111738. https://doi.org/10.1016/j.rser.2021.111738.
2. Zaboli M, Ajarostaghi SSM, Saedodin S, Pour MS. Thermal performance enhancement using absorber tube with inner helical axial fins in a parabolic trough solar collector. Appl Sci. 2021;11:7423. https://doi.org/10.3390/app11167423.
3. Bhakre S, Sawarkar P, Kalamkar V. Performance evaluation of PV panel surfaces exposed to hydraulic cooling–a review. Sol Energy. 2021;224:1193–209. https://doi.org/10.1016/j.solener.2021.06.083.
4. Alshuraiaan B. Evaluation of the thermal performance of various nanofluids used to harvest solar energy. Energy Ecol Environ. 2021;6:531–9.
5. Saedodin S, Zaboli M, Ajarostaghi SSM. Hydrothermal analysis of heat transfer and thermal performance characteristics in a parabolic trough solar collector with turbulence-inducing elements. Sustain Energy Technol Assess. 2021;46:101266. https://doi.org/10.1016/j.seta.2021.101266.
6. Hossain F, Karim M, Bhuiyan A. A review on recent advancements of the usage of nano fluid in hybrid photovoltaic/thermal (PV/T) solar systems. Renew Energy. 2022;188:114–31. https://doi.org/10.1016/j.renene.2022.01.116.
7. Zaytseva O, Neumann G. Carbon nanomaterials: production, impact on plant development, agricultural and environmental applications. Chem Biol Technol Agric. 2016;3:17. https://doi.org/10.1186/s40538-016-0070-8.
8. Wahab A, Khan M, Hassan A. Impact of graphene nanofluid and phase change material on hybrid photovoltaic thermal system: exergy analysis. J Clean Prod. 2020;277:123370. https://doi.org/10.1016/j.jclepro.2020.123370.
9. Qeays I, Yahya S, Asjad M, Khan Z. Multi-performance optimization of nanofluid cooled hybrid photovoltaic thermal system using fuzzy integrated methodology. J Clean Prod. 2020;256:120451. https://doi.org/10.1016/j.jclepro.2020.120451.
10. Parsa S, Yazdani A, Aberoumand H, Farhadi Y, Ansari A, Aberoumand S, Karimi N, Afrand M, Cheraghian G, Ali H. A critical analysis on the energy and exergy performance of photovoltaic/thermal (PV/T) system: the role of nanofluids stability and synthesizing method. Sustain Energy Technol Assess. 2022;51:101887. https://doi.org/10.1016/j.seta.2021.101887.
11. Kim S, Choi S, Kim D. Thermal conductivity of metal-oxide nanofluids: particle size dependence and effect of laser irradiation. J Heat Transf. 2007;129:298–307.
12. Delouei A, Sajjadi H, Izadi M, Mohebbi R. The simultaneous effects of nanoparticles and ultrasonic vibration on inlet turbulent flow: an experimental study. Appl Therm Eng. 2019;146:268–77.
13. Abdallah S, Elsemary I, Altohamy A, Abdelrahman M, Attia A, Abdellatif O. Experimental investigation on the effect of using

nano fluid (Al_2O_3-Water) on the performance of PV/T system. Therm Sci Eng Prog. 2018;7:1–7.
14. Yang L, Hu Y. Toward TiO_2 nanofluids—part 1: preparation and properties. Nanoscale Res Lett. 2017;12:417. https://doi.org/10.1186/s11671-017-2184-8.
15. Kiliç F, Menlik T, Sözen A. Effect of titanium dioxide/water nanofluid use on thermal performance of the flat plate solar collector. Sol Energy. 2018;164:101–8.
16. Subramani J, Nagarajan P, Mahian O, Sathyamurthy R. Efficiency and heat transfer improvements in a parabolic trough solar collector using TiO_2 nanofluids under turbulent flow regime. Renew Energy. 2018;119:19–31.
17. Kahani M, Zamen M, Rostami B. Modeling and empirical study of TiO_2/water nanofluid flows in a modified configuration with new layer arrangement of a photovoltaic/thermal system. Sustain Energy Technol Assess. 2022;51:101932. https://doi.org/10.1016/j.seta.2021.101932.
18. Zaboli M, Ajarostaghi SSM, Saedodin S, Behnam K. Hybrid nanofluid flow and heat transfer in a parabolic trough solar collector with inner helical axial fins as turbulator. Eur Phys J Plus. 2021;136:841. https://doi.org/10.1140/epjp/s13360-021-01807-z.
19. Samylingam L, Aslfattahi N, Saidur R, Yahya S, Afzal A, Arifutzzaman A, Tan K, Kadirgama K. Thermal and energy performance improvement of hybrid PV/T system by using olein palm oil with MXene as a new class of heat transfer fluid. Solar Energy Mater Solar Cells. 2020;218:110754. https://doi.org/10.1016/j.solmat.2020.110754.
20. Yan S, Kalbasi R, Nguyen Q, Karimipour A. Rheological behavior of hybrid MWCNTs-TiO_2/EG nanofluid: a comprehensive modeling and experimental study. J Mol Liq. 2020;308:113058.
21. Sangeetha M, Manigandan S, Ashok B, Brindhadevi K, Pugazhendhi A. Experimental investigation of nanofluid based photovoltaic thermal (PV/T) system for superior electrical efficiency and hydrogen production. Fuel. 2021;286:119422.
22. Venkatesh T, Manikandan S, Selvam C, Harish S. Performance enhancement of hybrid solar PV/T system with graphene based nanofluids. Int Commun Heat Mass Transfer. 2022;130:105794.
23. Shankara R, Banapurmath N, D'Souza A, Sajjan A, Ayachit N, Khan T, Badruddin I, Kamangar S. An insight into the performance of radiator system using ethylene glycol-water based graphene oxide nanofluids. Alex Eng J. 2022;61:5155–67. https://doi.org/10.1016/j.aej.2021.10.037.
24. Bahiraei M, Heshmatian S. Graphene family nanofluids: a critical review and future research directions. Energy Convers Manage. 2019;196:1222–56.
25. Chiam HW, Azmi WH, Usri NA, Mamat R, Adam NM. Thermal conductivity and viscosity of Al_2O_3 nanofluids for different based ratio of water and ethylene glycol mixture. Exp Thermal Fluid Sci. 2017;81:420–9. https://doi.org/10.1016/j.expthermflusci.2016.09.013.
26. Esfe MH, Razi P, Hajmohammad MH, Rostamian SH, Sarsam WS, Arani AAA, Dahari M. Optimization, modeling and accurate prediction of thermal conductivity and dynamic viscosity of stabilized ethylene glycol and water mixture Al_2O_3 nanofluids by NSGA-II using ANN. Int Commun Heat Mass Transfer. 2017;82:154–60.
27. Adun H, Kavaz D, Dagbasi M. Review of ternary hybrid nanofluid: synthesis, stability, thermophysical properties, heat transfer applications, and environmental effects. J Cleaner Prod. 2021;328:129525. https://doi.org/10.1016/j.jclepro.2021.129525.
28. Tiwari AK, Kumar V, Said Z, Paliwal HK. A review on the application of hybrid nanofluids for parabolic trough collector: recent progress and outlook. J Cleaner Prod. 2021;292:126031. https://doi.org/10.1016/j.jclepro.2021.126031.
29. Sandhya M, Ramasamy D, Sudhakar K, Kadirgama K, Samykano M, Harun WSW, Najafi G, Mofijur M, Mazlan M. A systematic review on graphene-based nanofluids application in renewable energy systems: preparation, characterization, and thermophysical properties. Sustain Energy Technol Assess. 2021;44:101058. https://doi.org/10.1016/j.seta.2021.101058.
30. Sati P, Shende RC, Ramaprabhu S. An experimental study on thermal conductivity enhancement of DI water-EG based ZnO(CuO)/graphene wrapped carbon nanotubes nanofluids. Thermochim Acta. 2018;666:75–81. https://doi.org/10.1016/j.tca.2018.06.008.
31. Sunil J, Vignesh J, Vettumperumal R, Maheswaran R, Raja RAA. The thermal properties of CaO-nanofluids. Vacuum. 2019;161:383–8. https://doi.org/10.1016/j.vacuum.2019.01.010.
32. Fazal MA, Rubaiee S. Progresses of PV cell technology: feasibility of building materials, cost, performance, and stability. Sol Energy. 2023;258:203–19. https://doi.org/10.1016/j.solener.2023.04.066.
33. Rubaiee S, Fazal MA. Efficiency enhancement of photovoltaic solar system by integrating multi-pipe copper frame filled with ZnO doped phase change material. MRS Energy Sustain. 2023. https://doi.org/10.1557/s43581-023-00063-1.
34. Rahman MM, Hasanuzzamana M, Rahim NA. Effects of operational conditions on the energy efficiency of Photovoltaic modules operating in Malaysia. J Clean Prod. 2017;143:912–24. https://doi.org/10.1016/j.jclepro.2016.12.029.
35. Nasrin R, Hasanuzzaman M, Rahim NA. Effect of nanofluids on heat transfer and cooling system of the photovoltaic/thermal performance. Int J Numer Method H. 2019;2019(29):1920–46. https://doi.org/10.1108/HFF-04-2018-0174.